

Research Article

Effect of Nanoaluminium Nitride Ceramic Particles on Microstructure, Mechanical Wear, and Machining Behavior of Al-Si-Mg Alloy Matrix Composites Produced by Bottom Pouring Type Stir Casting Route

M. Meignanamoorthy,¹ V. Mohanavel ,² P. Velmurugan ,² M. Ravichandran ,¹ Wadi B. Alonazi ,³ S. Sivakumar,⁴ and Atkilt Mulu Gebrekidan ⁵

¹Department of Mechanical Engineering, K. Ramakrishnan College of Engineering, Tiruchirappalli, 621112 Tamil Nadu, India

²Centre for Materials Engineering and Regenerative Medicine, Bharath Institute of Higher Education and Research, Selaiyur, Chennai, 600073 Tamil Nadu, India

³Health Administration Department, College of Business Administration, King Saud University, PO Box 71115, Riyadh 11587, Saudi Arabia

⁴Department of Bioenvironmental Energy, College of Natural Resource and Life Science, Pusan National University, Miryang 50463, Republic of Korea

⁵Department of Mechanical Engineering, Faculty of Mechanical Engineering, Arba Minch Institute of Technology (AMIT), Arba Minch University, Ethiopia

Correspondence should be addressed to Atkilt Mulu Gebrekidan; atkilt.mulu@amu.edu.et

Received 16 November 2021; Revised 22 December 2021; Accepted 24 December 2021; Published 3 February 2022

Academic Editor: Arpita Roy

Copyright © 2022 M. Meignanamoorthy et al. This is an open access article distributed under the Creative Commons Attribution License, which permits unrestricted use, distribution, and reproduction in any medium, provided the original work is properly cited.

Aluminium alloy strengthened with the ceramic particle is widely utilized for numerous engineering usages owing to its less weight, and superior mechanical and tribological behavior. The purpose of this research is to manufacture AA6063-Nano AlN composites via stir casting (SC) process and to examine the mechanical, tribological, electrical, and thermal and CNC drilling behavior. Nano AlN was mixed with AA6063 at 4, 8, and 12 wt.%. The occurrence and dispersal of Nano AlN particles in AA6063 matrix were inspected via Scanning Electron Microscope (SEM). The density and porosity were explored. The mechanical studies on microhardness, tensile strength and yield strength, flexural strength, and compressive strength have been done. SEM fractographic examination was made on the tensile fracture samples. The thermal conductivity, electrical resistivity and electrical conductivity, and salt spray corrosion analysis were made on the produced composites. The tribological behavior of the composites was studied using numerous parameters, reinforcement wt.%, load (L), sliding velocity (SV), and sliding distance (SD). The worn surface examination was done via SEM. The CNC drilling behavior was done at different parameter speed (S), feed (F), and depth of cut (DOC). Experiments were carried out according to the L9 orthogonal array (OA). Optimal process parameter to attain higher material removal rate (MRR) and least surface roughness (SR) was identified via Grey Relational Analysis (GRA). ANOVA outcomes revealed that feed rate is the foremost noteworthy parameter (45.89%) influencing MRR and SR.

1. Introduction

Nowadays, metal matrix composites (MMC) reinforced with ceramics have progressed as noteworthy focuses despite

their progressive usages equivalent to the traditional alloys. Because of their excellent properties, MMCs are largely utilized for different applications than traditional alloys [1]. MMCs can be finely strengthened with another material to

enhance their properties. In MMCs, the alloy or metal is a matrix phase and the reinforcement could be ceramic or organic. Generally, metal is an important one for numerous engineering applications; however, many attempts have been put forth to improve its properties via utilizing appropriate reinforcements [2, 3]. MMCs strengthened with particulates are majorly utilized in various engineering fields' aircraft and structural parts because of their higher strength, good toughness, better wear and corrosion opposition, etc. [4]. Currently, aluminium matrix composites (AMCs) are a majorly utilized material in various engineering fields. Aluminium is a lightweight metal, but it possesses poor mechanical properties. Furthermore, to improve the mechanical property of aluminium, it is reinforced with different kinds of ceramics. Hence, the desired properties can be attained [5]. Numerous engineering components need good strength, hardness, and wear and corrosion resistance materials with less weight. Despite this intention, aluminium is mixed with harder ceramic particles via a liquid metallurgy process to manufacture AMCs [6]. AMCs have aluminium or alloy as a matrix; nowadays, the usage of these AMCs has been enhanced in industry because of their superior properties. Because of these merits, aluminium alloy is combined with different reinforcements to obtain explicit properties [7]. Amid the numerous ceramics, AlN has been accredited as a superior one because it exhibits better mechanical, wear, corrosion, and thermal properties [8]. Due to better wettability and higher stability tendency of AlN with aluminium, it is attracted much more than other ceramics; additionally, AlN has good hardness and elastic modulus [9]. Several fabrication routes are available to prepare MMC hot pressing, PM, and stir casting. Amongst the different processes, stir casting (SC) has been identified as a major operative one despite its easiness, litness, large capacity, fabrication capability, and economical [10]. SC process confirms the fine dispersal of reinforcements with the aid of a stirrer. The strength of interfacial closeness amid reinforcement and alloys depends on wettability, because it is a noteworthy factor, which results in extreme enhancement of tribological and mechanical properties [11]. Chellapilla et al. [12] developed TiC strengthened AA6063 composites via in situ process and stated that inclusion of TiC with AA6063 enhances the composite properties. David Joseph et al. [12] produced MoS₂ reinforced AA6063 composites via PM route and concluded that the addition of MoS₂ to AA6063 enhances the material property. Saravanan et al. [13] synthesized TiC reinforced AA6063 matrix composites via the SC method, and the outcomes displayed that particle-reinforced AMCs increase the mechanical properties extremely. Mohanavel et al. [14] examined the AlN strengthened AA7075 composite mechanical behavior prepared via SC process and described that the increment of AlN reinforcement with matrix increases the properties significantly. Ashok Kumar et al. [15] explored the tribological behavior of AlN strengthened AA6061 composite and the results showed that a raise in AlN particles rises the wear opposition. Zhao et al. [16] manufactured AA6061-AlN composites by SC process and studied the mechanical behavior, and the outcomes explored

that the inclusion of reinforcement particles improves the properties. Mahesh Kumar et al. [17] analyzed the mechanical properties of AA7079-AlN composites prepared via SC route and stated that an increase in AlN wt.% enhances the properties of the composites. Fale et al. [18] explored the tensile, compressive, and wear behavior of Al-AlN composites prepared via ex situ process and stated that inclusions of AlN particles enhance the compressive and tensile strength and increase the wear resistance. Shalaby and Churyumov [19] fabricated AlN strengthened with A359 composites and the outcomes displayed that a rise in AlN wt.% improves the mechanical properties. Radhika and Raghu [20] explored the hardness, tensile strength, and abrasion wear behavior of Al-AlN composites and reported that dramatic improvement in properties was achieved due to the addition of AlN particles. Radhika and Raghu [21] studied the tensile strength; hardness and wear behavior of AlN strengthened LM13 composite and indicated that the inclusion of AlN particles enhances the properties of the composites significantly. Basavarajappa et al. [22] studied the drilling characteristics of AA2219-15SiC-3Gr composites prepared via SC route and burr height, thrust force, and surface roughness that were analyzed. Rajmohan and Palanikumar [23] explored the CNC drilling characteristics of Al356-SiC composites and concluded that the feed rate is a major significant parameter to affect the thrust force, burr height, tool wear, and surface roughness. Rajmohan et al. [24] investigated the CNC drilling parameters of Al356-SiC-mica composites, and the results revealed that the feed rate and addition of reinforcement wt.% were the major noteworthy parameters. Elango and Annamalai [25] examined the CNC machining characteristics of Al-SiC-Gr composites, and the results showed that cutting speed is the major influencing parameter to attain least surface roughness. Yahya Altunpak et al. [26] explored the drilling characteristics of aluminium composites, and the outcomes showed that the feed rate is the most substantial one to attain the least surface roughness.

Till now, various examinations have been conducted to study the mechanical, tribological, and CNC drilling behavior of AMC-based composites, but very little work has been done by utilizing Nano AlN particles as reinforcement. Therefore, this work made an effort to manufacture AA6063-Nano AlN composites via the SC process and studied the behavior of the prepared composites.

2. Materials and Methods

AA6063 chemical compositions are Si:0.2-0.6, Fe:0.35, Cu:0.1, Mn:0.1, Mg:0.45-0.9, Zn:0.1, Ti:0.1, Cr:0.1, and Al:Balance. AA6063 was preferred as matrix and Nano AlN (4, 8, and 12 wt.%) as reinforcement. The desired amount of AA6063 and Nano AlN was measured via electronic weighing equipment. AA6063 was liquefied at 750°C temperature [27]. Nano AlN particle was preheated at 400°C before being added into the liquefied metal [14]. The least amount of magnesium was added to raise the wettability [28]. Stirring was conducted at 400 rpm for 15 min [17]. Finally, the molten metal was transferred into a mould of

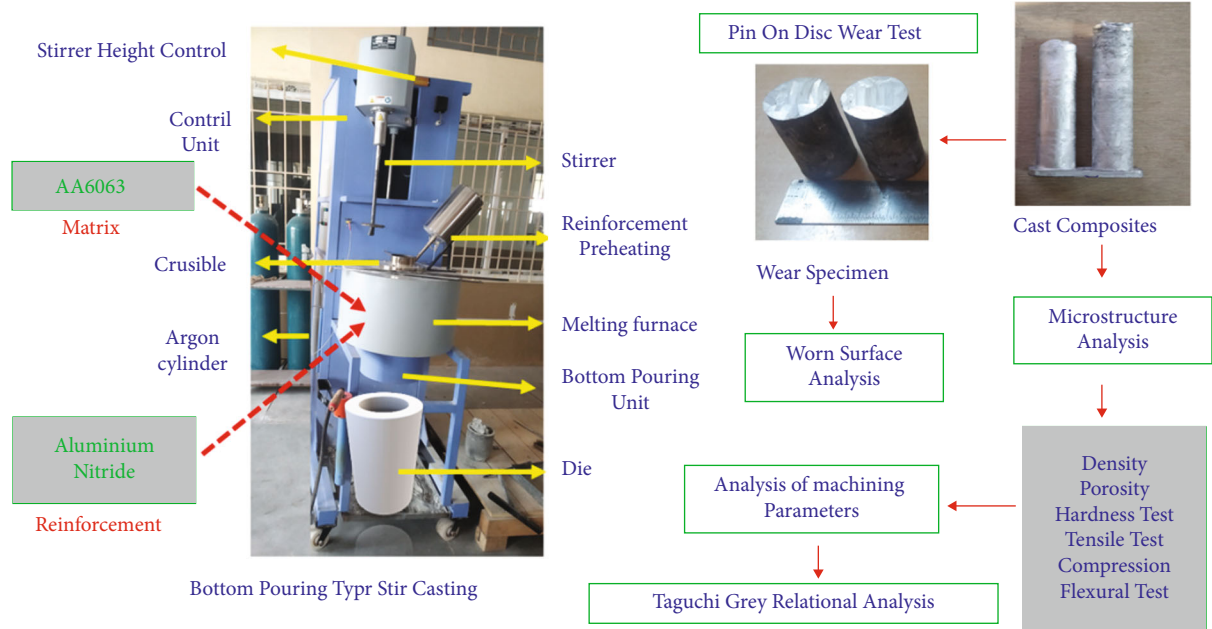


FIGURE 1: Experimental details of the present work.

the requisite dimensions. Microstructure exploration was made via SEM on the manufactured samples. By utilizing Archimedes' principle, the density was calculated and porosity was also measured. The prepared samples' hardness was determined as per ASTM E92 using a Vickers hardness machine [29]. According to ASTM E8–04 standard, a tensile test was done using computerized universal testing equipment [29]. As per ASTM E9-89a, a compression test was done utilizing computerized universal testing equipment [30]. The flexural strength was conducted according to ASTM standard C1161 via three-point bending equipment [13]. The thermal conductivity analysis was done at room temperature via a thermal diffusivity analyzer. Electrical conductivity examination was done via the four-point probe technique. According to ASTM B, the 117 standard salt spray corrosion test was conducted utilizing a salt spray chamber in 5% NaCl for 72 hours. Later, the specimens are washed with water and air-dried up before measuring weight loss. The tribological behavior of the prepared composites was analyzed concerning ASTM G99 via a pin-on-on-a-disc instrument (Ducom Instruments Pvt Ltd). The parameters for tribological experimentation are (1) speed of 300 rpm, (2) time of 1000 s, and (3) sliding velocity 0.5–2.0 m/s at an interval of 0.5. The CNC drilling process was done using Siemens CNC lathe (MTAB) to analyze the MRR and SR. The MRR was found by determining the weight of samples previously and later machining, and SR was measured using the surface roughness tester TR110. Overall, the experimental scheme is given in Figure 1.

3. Results and Discussion

3.1. SEM Examination of Composites. Figures 2(a)–2(d) show the SEM images of AA6063-4wt.%Nano AlN, AA6063-8wt.%Nano AlN, and AA6063-12wt.%Nano AlN

composites. Figures 2(b)–2(d) display the occurrence and even dispersal of Nano AlN particles in the AA6063 matrix. From the SEM images (Figures 2(b)–2(d)), while increasing the wt.% from 4 to 12, more amount of particle dispersal can be seen in Figure 2(d); it indicates that fine dispersal was attained in the composites. Furthermore, no voids, cracks, pores, and clustering of particles are witnessed in any of the composites. The composites possess good bonding amid matrix and particle; this is owing to the matrix boundary that becomes hardened initially; then, Nano AlN reinforcement left out via solid/liquid boundary which leads Nano AlN particles becomes separated at the interdendrite zone [17].

3.2. Density and Porosity Analysis. Figure 3 displays the density and porosity examination of AA6063-Nano AlN composites. From Figure 3, it is clear that experimental density is lesser than the theoretical density when increasing the reinforcement from 0 to 12 wt.%. The increment in theoretical density is due to the hard tendency of Nano AlN particles and additionally excellent bonding occurred amid the matrix and reinforcement. It is witnessed from the SEM images (Figures 2(b)–2(d)). Furthermore, the density of Nano AlN is higher than that of AA6063, this might be one of the reasons for density enhancement. While increasing the wt.% of Nano AlN from 4 to 12, the porosity of the composites reduced gradually; this is because no pores, voids, and cracks were found in any of the composites; it is clear from the SEM images (Figures 2(a)–2(d)).

Due to the selection of suitable stir casting process parameters, uniform dispersal of reinforcement and matrix was occurred.

3.3. Influence of Nano AlN on Microhardness. The influence of Nano AlN wt.% on microhardness was studied, and

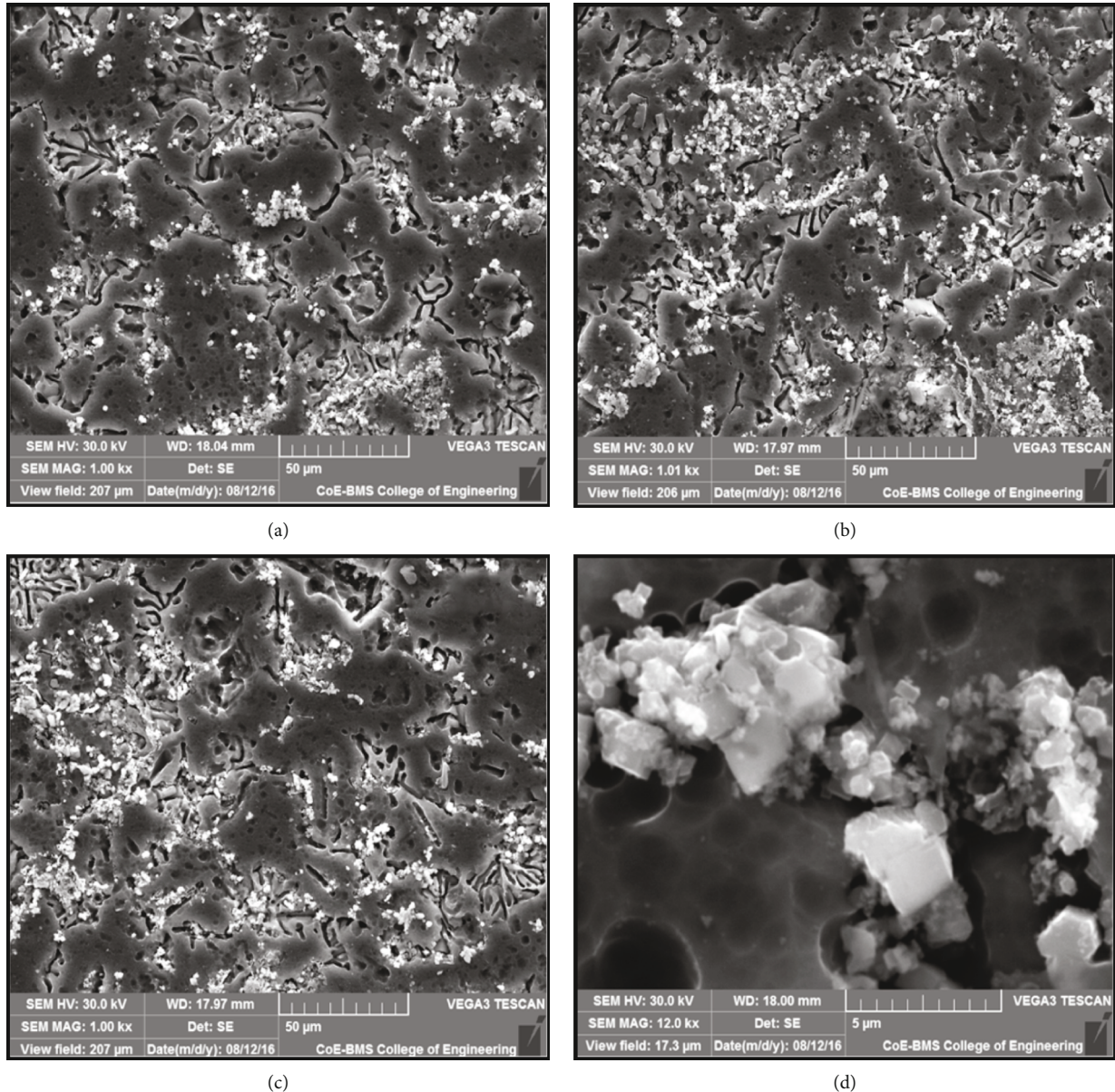


FIGURE 2: (a–d) SEM images of AA6063-4wt.%Nano AlN, AA6063-8wt.%Nano AlN, and AA6063-12wt.%Nano AlN.

Figure 4 shows the AA6063-Nano AlN composites microhardness. The microhardness of AA6063-Nano AlN composites was enhanced when increasing the Nano AlN wt.% from 4 to 12. This is owing to the high hardness of Nano AlN particles than the AA6063 matrix and proper bonding amid the matrix and reinforcement; it is witnessed by SEM images (Figures 2(b)–2(d)). Despite grain enhancement, the particle strengthening and load-bearing ability of hard reinforcement particle to matrix hardness of the composites improved. The surface area was improved due to inclusion of Nano AlN reinforcement into AA6063 matrix; additionally, the grain size of the matrix was reduced. However, more amount of reinforcement in the matrix hints to improved dislocation density all through the solidification owing to the thermal absurdity amid the matrix and reinforcement [17]. The least hardness attained was 64 HV for the

AA6063 matrix, and the higher hardness attained was 92 HV for the composites AA6063-12 wt%. Nano AlN. The 30.43% of improvement in hardness was achieved when 12 wt% of Nano AlN were added to AA6063 matrix.

3.4. Influence of Nano AlN on Tensile and Yield Strength.

The effect of Nano AlN wt.% on the tensile and yield strength of AA6063 matrix composites is shown in Figure 5. It is witnessed that AA6063 matrices possess the least tensile and yield strength than that of AA6063-Nano AlN composites. From Figure 5, it is clear that increasing the Nano AlN wt.% from 4 to 12, a gradual enhancement in tensile and yield strength was attained. The various reasons for the enhancement in tensile strength are the grain refinement obtainable via Nano AlN; Nano AlN particles act as obstacles to the motion of displacements which results

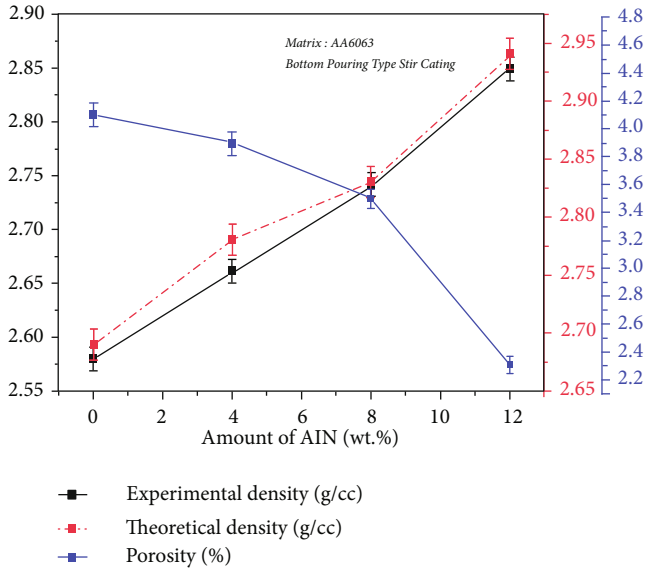


FIGURE 3: Experimental and theoretical densities and porosity of AA6063-Nano AlN composites.

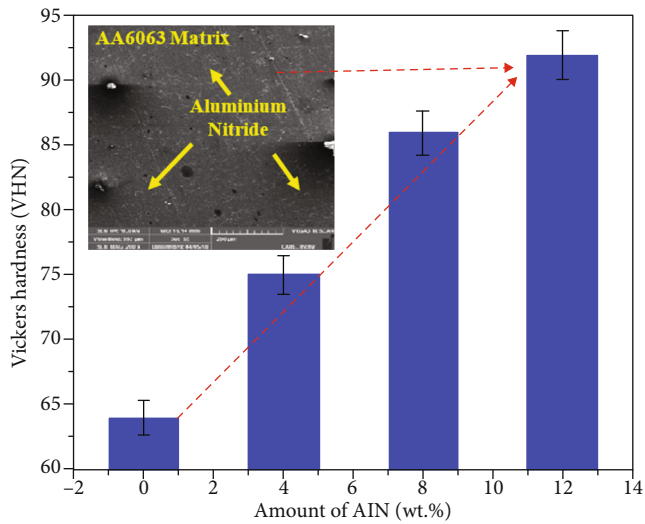


FIGURE 4: Microhardness of AA6063-Nano AlN composites and inset shows the SEM image of the composite sample with uniform distribution of Nano AlN particles.

in enhanced tensile strength [14]. Even the dispersal of Nano AlN takes the conversion of smeared load from matrix to Nano AlN particles; moreover, coefficient of thermal development amid matrix reinforcement originates an enormous amount of dislocation density about the surface of reinforcement particles, and the one major reason is dispersal strengthening mechanism [8]. The lowest ultimate tensile strength attained was 13.51 MPa for AA6063 matrix, and the extreme ultimate tensile strength obtained was 297.21 MPa for the AA6063-12wt.%Nano AlN composites. The 54.4% of enhancement in ultimate tensile strength was attained when 12 wt.% of Nano AlN were added to AA6063 matrix.

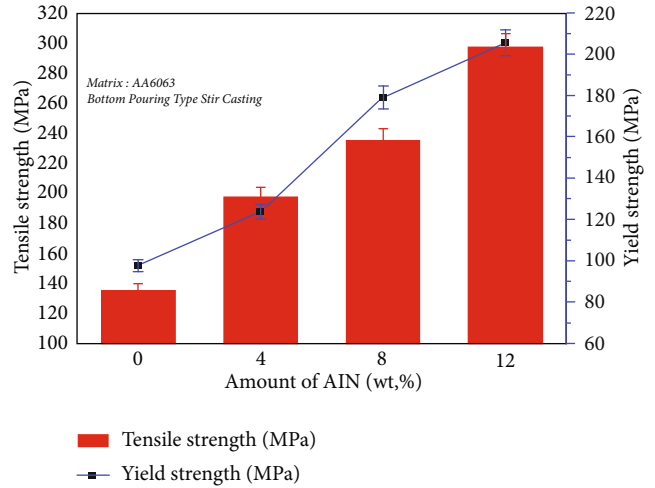


FIGURE 5: Tensile and yield strength of AA6063-Nano AlN composites.

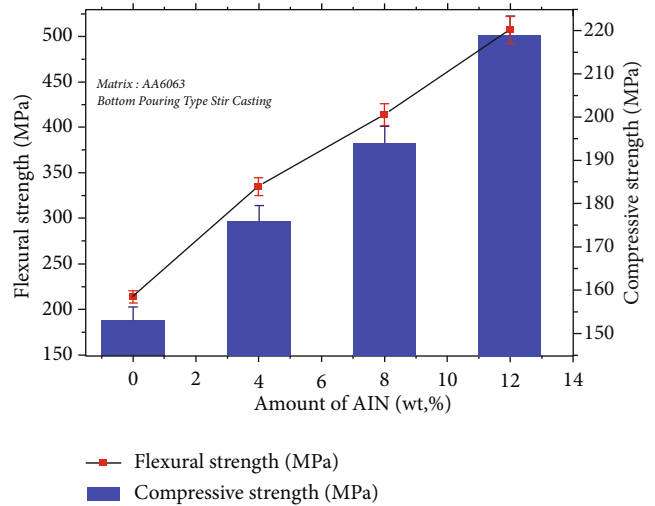


FIGURE 6: Compressive and flexural strength of AA6063-Nano AlN composites.

Figure 5 displays yield strength (YS) of AA6063-Nano AlN composite. Figure 5 surely displays that AA6063 matrix exhibits the least yield strength after the addition of Nano AlN particle to AA6063 matrix increase in YS of the produced composites acquired. The occurrence of Nano AlN particles in matrix frontrunners due to diminished matrix grain size. Reference to Hall-Petch correlation yield strength is in reverse relational with grain size. Likewise, yield strength of the AA6063-Nano AlN composites rises [14]. The least yield strength 97.59 MPa was attained for AA6063 matrix, and the maximum yield strength 205.60 was attained for the AA6063-12wt.%Nano AlN composites.

3.5. Influence of Nano AlN on Compressive Strength. The influence of Nano AlN wt.% on the compressive strength of AA6063 matrix composites is shown in Figure 6. It is observed that AA6063 matrix exhibits minimum

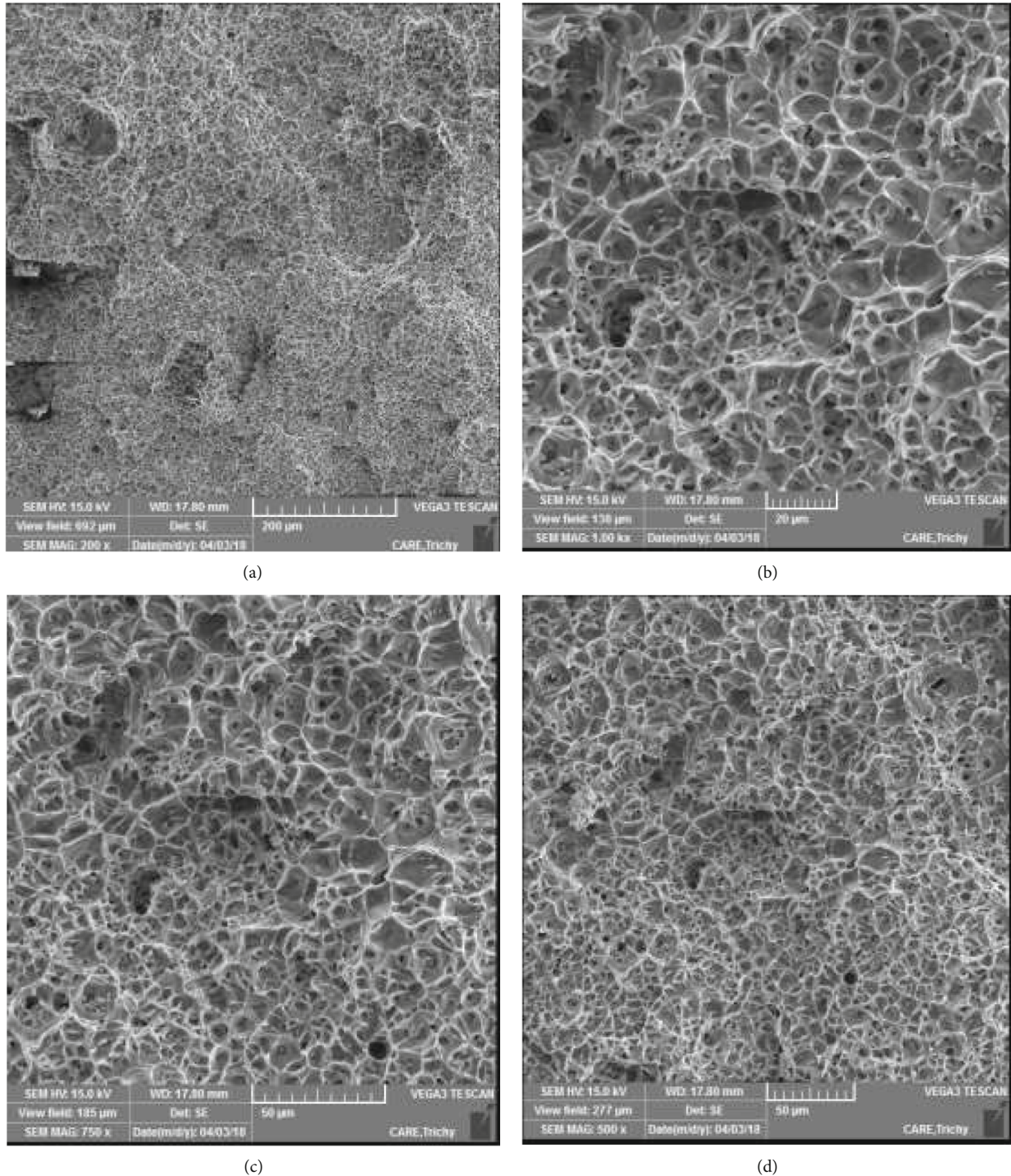


FIGURE 7: Tensile fracture surface of AA6063, AA6063-4 wt.%Nano AlN, AA6063-8 wt.%Nano AlN, and AA6063-12 wt.%Nano AlN composites.

compressive strength than that of AA6063-Nano AlN composites. From Figure 6, it can be understood that a raise in Nano AlN wt.% from 4 to 12 an enhancement in compressive strength was obtained. The existence of Nano AlN particles in matrix performs as a hindrance to the movement of dislocation pointer with an additional enhancement in compression strength. The enhanced dislocation instigated via

CTE divergence is one of the reasons for the increment in compression strength. The major important reason for compressive strength enhancement is the fine and even scattering of Nano AlN particles in matrix [31]. The lowest compressive strength achieved was 153 MPa for AA6063 matrix, and the extreme compressive strength attained was 219 MPa for the composites AA6063-12wt.%Nano AlN.

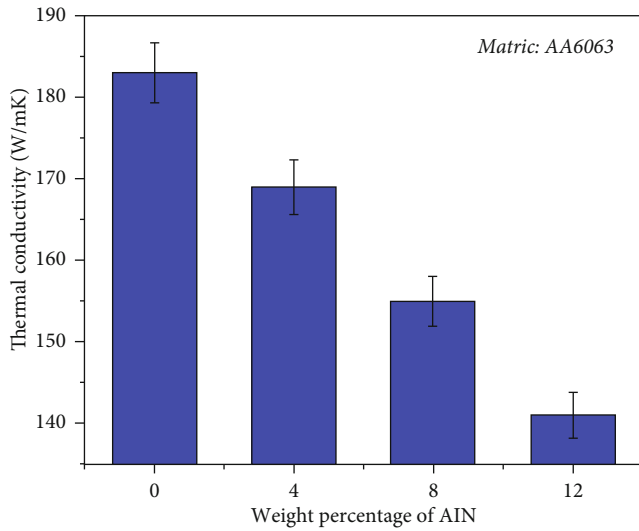


FIGURE 8: Thermal conductivity of AA6063-Nano AlN composites.

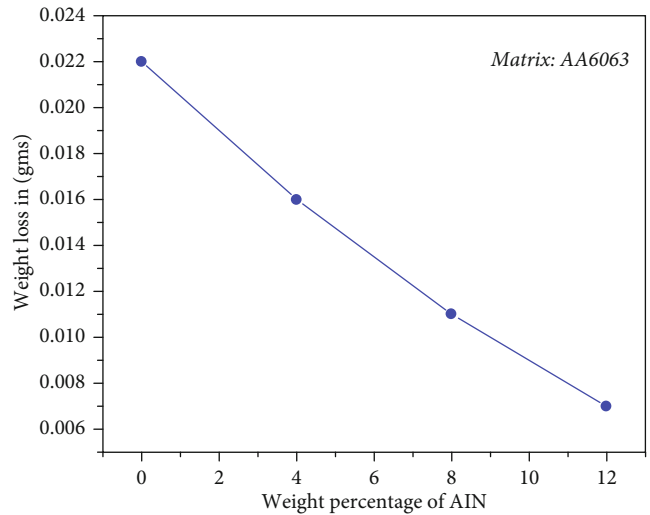


FIGURE 10: Effect of Nano AlN on wear properties.

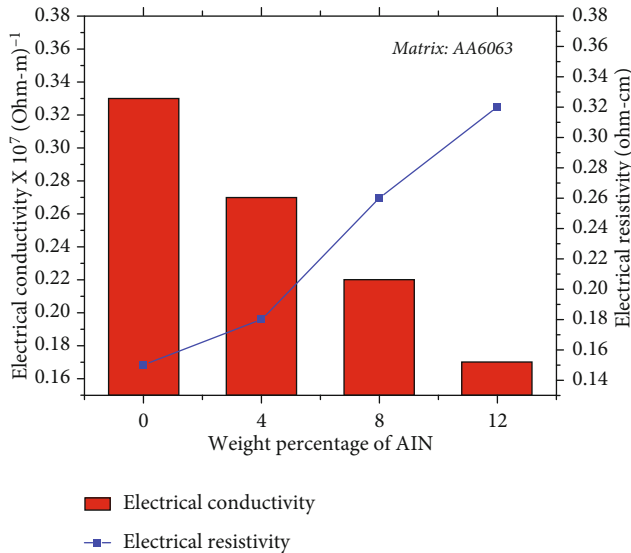


FIGURE 9: Thermal conductivity of AA6063-Nano AlN composites.

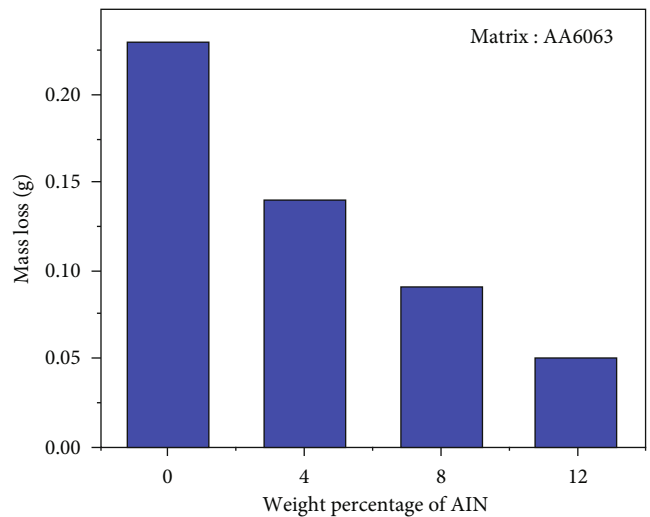


FIGURE 11: Salt spray corrosion of AA6063-Nano AlN composites.

Therefore, it can be clearly implicit that 12 wt.%Nano AlN composites possess superior strength than that of the unreinforced alloy.

The influence of Nano AlN wt.% on the flexural strength of AA6063 matrix composites was shown in Figure 6. It is detected that AA6063 matrix exhibits the least flexural strength than that of AA6063-Nano AlN composites. From Figure 6, it is clear that the increment in Nano AlN wt.% from 4 to 12 results in increased flexural strength. This may be ascribed to an enhanced dislocation density triggered via thermal coefficient growth conflict amid the matrix and reinforcement, which results in the improvement of the flexural strength [32]. Besides, the boundary amid matrix and Nano AlN reinforcement transports the load from the matrix to reinforcement particle outstandingly.

3.6. SEM Examination of Tensile Fractures. Figures 7(a)–7(d) show tensile fracture of AA6063 and AA6063-Nano AlN composites. Figure 7(a) clearly shows the large dimples, this dimple formation is despite of the ductile nature of the AA6063 matrix, and Figure 7(a) specifies that uniformly dispersed voids display a ductile nature. From Figures 7(b)–7(d), it might be implicit that the void sizes of the produced AA6063-Nano AlN composites are smaller when compared to the matrix alloy (Figure 7(a)). The fractured surface represents a moderately flat presence, which shows macroscopically breakable fractures and microscopically malleable fractures. A smaller void formation occurred when the Nano AlN particles reinforced with AA6063 matrix, which developed the grain size and ductility decreased. Furthermore, it is witnessed that Nano AlN particles left over the whole in

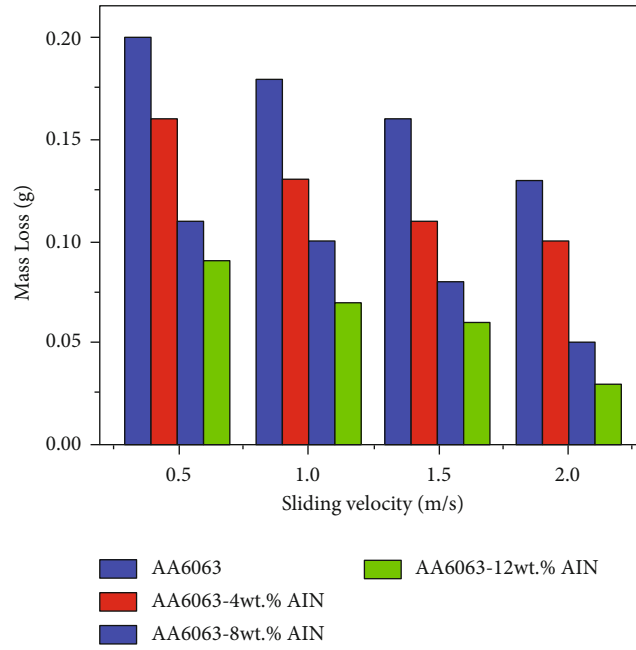


FIGURE 12: Plot between sliding velocity and mass loss.

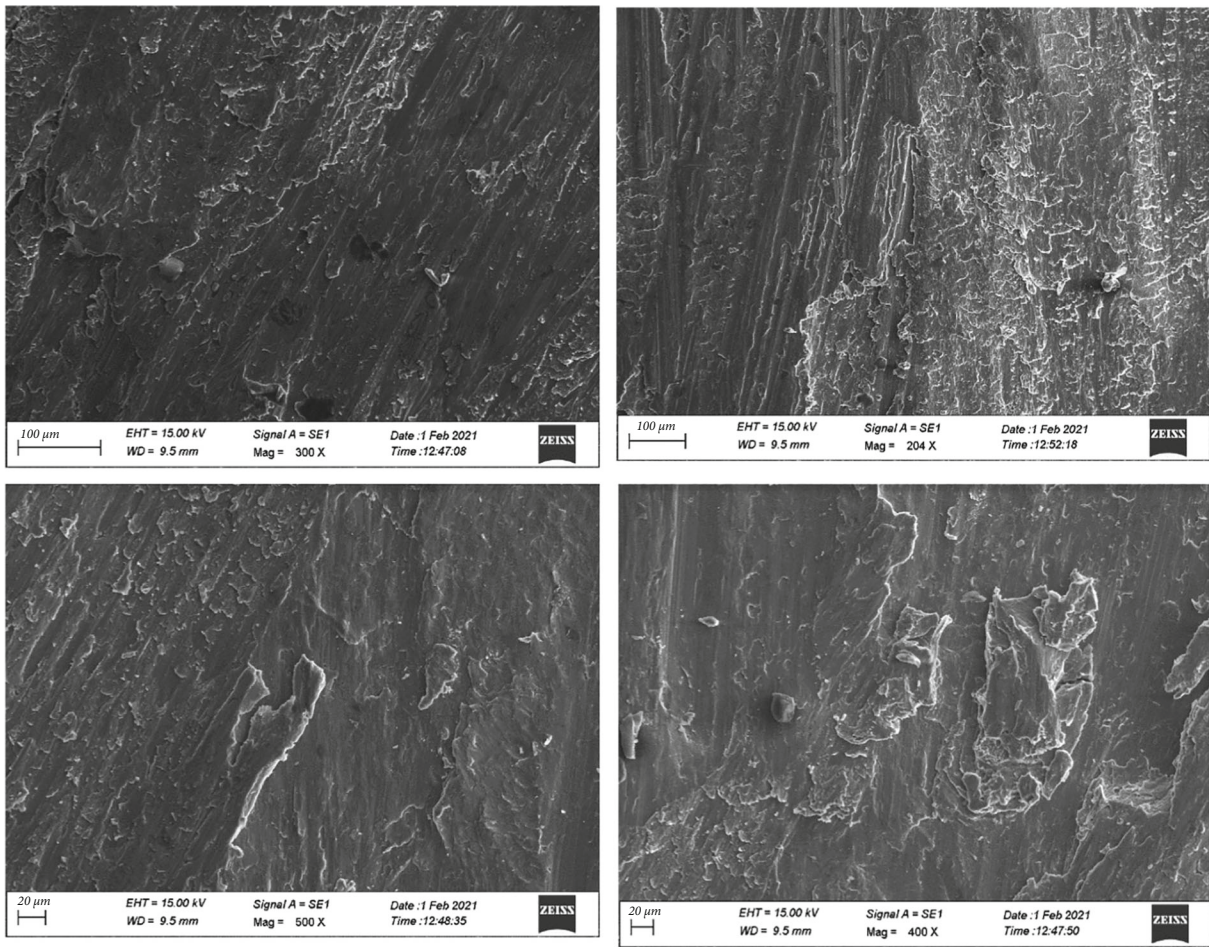


FIGURE 13: Worn surface analysis of AA6063, AA6063-4wt.%Nano AlN, AA6063-8wt.%Nano AlN, and AA6063-12wt.%Nano AlN composites.

TABLE 1: Input parameters and output results.

Ex. No	CS (rpm)	FR (mm/rev)	DOC (mm)	MRR (g/min)	SR (μm)
1	1000	0.05	0.2	0.073	1.88
2	1000	0.15	0.3	0.097	1.68
3	1000	0.25	0.4	0.118	1.75
4	2000	0.05	0.3	0.081	2.02
5	2000	0.15	0.4	0.104	2.25
6	2000	0.25	0.2	0.124	2.09
7	3000	0.05	0.4	0.09	2.17
8	3000	0.15	0.2	0.112	1.59
9	3000	0.25	0.3	0.147	1.80

some locations on the fracture surface, which provides confirmation for the occurrence of enhanced bonding amid AA6063 matrix and reinforced Nano AlN particles.

3.7. Thermal Conductivity. The influence of Nano AlN particles on the thermal conductivity of AA6063 matrix is shown in Figure 8. The addition of Nano AlN to AA6063 reduces the thermal conductivity. The AA6063-Nano AlN composite thermal conductivity reduces while adding wt.% from 4 to 12. The thermal conductivity of the composites is commonly pretentious by weight percentage and kind of reinforcement, density, or porosities, and fabrication routes utilized are vital factors, which affect the thermal conductivity values. However, in this investigation, it is clear that the thermal conductivity of AA6063 matrix is higher than Nano AlN particle, and this is the major cause for the decline in the composite thermal conductivity. Therefore, the inclusion of Nano AlN with AA6063 furthermore declines the composite thermal conductivity. From the investigations, it is clear that 12 wt.%Nano AlN reinforced AA6063 composites possess less thermal conductivity when compared with other composites. The major cause might be interference of oxide particles could improve the mechanical properties. However, it reduces the thermal conductivity. The obtained outcomes are finely matched with the earlier results of different researchers [33, 34].

3.8. Electrical Conductivity. The effect of Nano AlN particles on the electrical resistivity and conductivity of AA6063 matrix is shown in Figure 9. It is clearly visible from Figure 9 that addition of Nano AlN to AA6063 improves the electrical resistivity. The major reason for the enhancement in electrical resistivity is grain size reduction. Simultaneously, the addition of Nano AlN to AA6063 decreases the electrical conductivity. The reason for the decline in electrical conductivity is despite of the oxidative nature of Nano AlN particles in addition to that Nano AlN particles possess less electrical conductive nature.

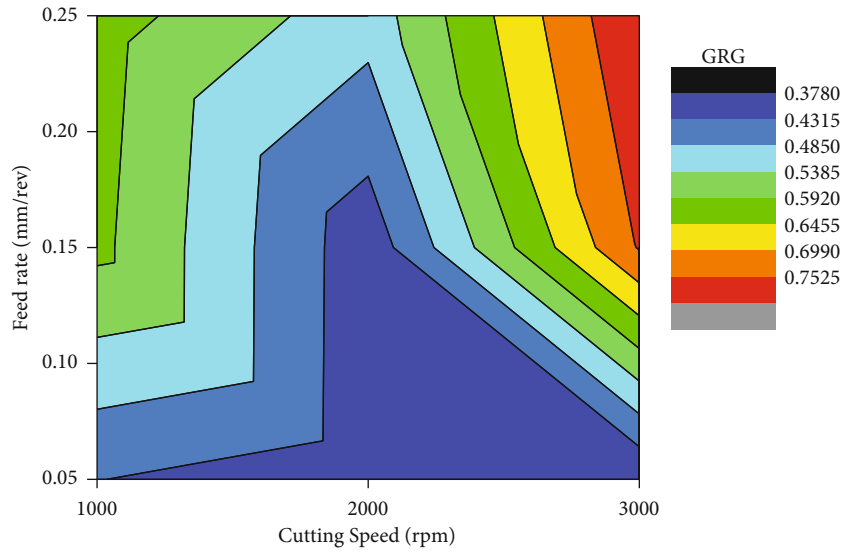
3.9. Salt Spray Corrosion Analysis. The effect of Nano AlN particles on the corrosion behavior of AA6063 matrix is shown in Figure 10. It is indeed noticeable from Figure 11 that inclusion of Nano AlN with AA6063 improves the corrosion resistivity of the composites. This is because of the

mechanical and hard nature of the Nano AlN particles. In addition to that, even distribution of Nano AlN particles in AA6063 matrix is also one of the reasons for the improved corrosion resistance which is clear from SEM analysis (Figures 2(a)–2(d)). While increasing the reinforcement weight percentage from 4 to 12, oxide layers formed over the AA6063 matrix surface reduced the weight loss. The oxide film guards the basic surface from extra corrosion outbreak [35]. Because of the above-mentioned reasons, the weight loss of AA6063-12wt.%Nano AlN composite is less when compared to other composites.

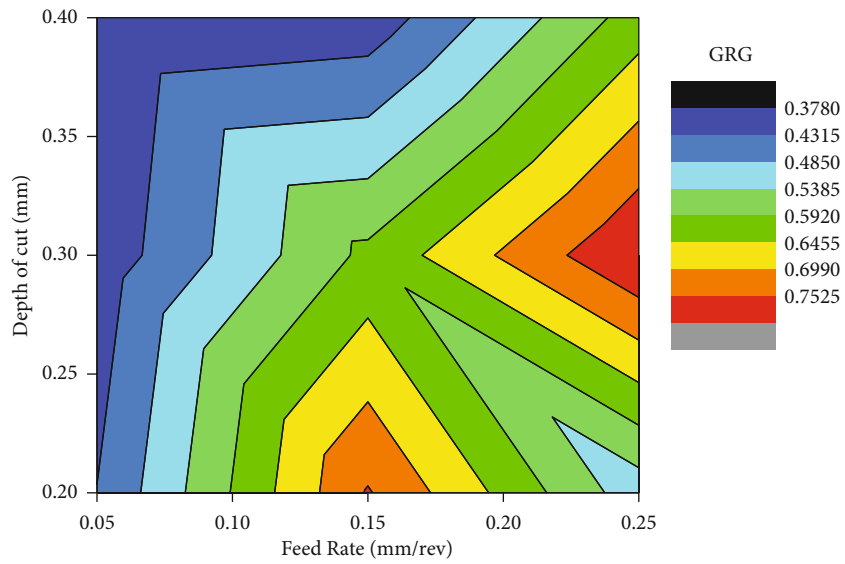
3.10. Tribological Analysis. Figures 10 and 12 display the influence of Nano AlN particles on the tribological behavior of the prepared composites. Figure 10 displays the wt.% of Nano AlN vs. mass loss amid wear analysis. AA6063 matrices attained higher mass loss, and 12 wt.% reinforced Nano AlN composites attain the least mass loss. It can be clearly witnessed that hard Nano AlN particles strengthened with AA6063 matrix lead to noteworthy enhancement in mass loss. It could be understood from the Archard equation that materials wear opposition is straightly linked to hardness [36]. From the obtained results, it is clear that the higher mass loss was attained for AA6063-12 wt.%Nano AlN composites and this is because of the effect of Nano AlN particle. The other major cause for the decline in mass loss while the wt.% range is despite of the greater hardness of Nano AlN particles. With reference to the rule of mixtures, a raise in hard reinforcement particles results in better wear opposition.

Figure 12 displays the graph for SV and mass loss of AA6063-Nano AlN composites. It is clear from the graph (Figure 9) that the decline in mass loss was obtained while increasing the SV from 0.5 to 1.5 m/s. Increment in mass loss for AA6063 was attained while increasing the SV up to 2 m/s. The cause for the enhancement in mass loss at a SV of 2 m/s might be owing to the maximum temperature expansion at maximum SV. However, the maximum temperature expansion reduces the stress and strain rate amid sliding [36].

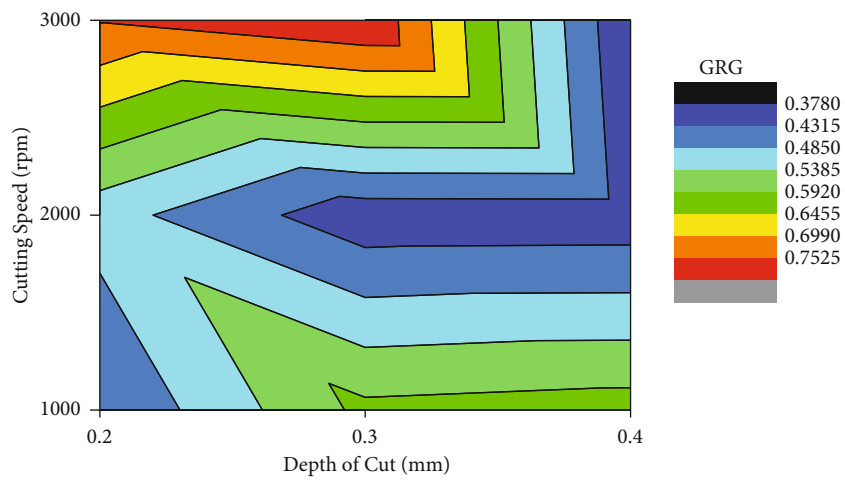
3.11. Worn Surface Examination. Figures 13(a)–13(d) show the worn surface examination of AA6063-Nano AlN composites. The SEM analysis of AA6063-Nano AlN composites displays some craters, grooves, pullouts, and plastic



(a)



(b)



(c)

FIGURE 14: (a) Contour plot for MRR and SR CS vs FR. (b) Contour plot for MRR and SR FR vs. CS. (c) Contour plot for MRR and SR DOC vs. CS.

TABLE 2: Normalized S/N ratio and deviation sequence.

Ex. No	Normalized S/N ratio		Deviation sequence	
	MRR	SR	MRR	SR
1	0	0.560606	1	0.439394
2	0.324324	0.863636	0.675676	0.136364
3	0.608108	0.757576	0.391892	0.242424
4	0.108108	0.348485	0.891892	0.651515
5	0.418919	0	0.581081	1
6	0.689189	0.242424	0.310811	0.757576
7	0.22973	0.121212	0.77027	0.878788
8	0.527027	1	0.472973	0
9	1	0.681818	0	0.318182

deformation. The Nano AlN particles occurred in the crater display few fragmented particles, and from the surface dragged out particles was found. The outcome specifies the abrasive wear mechanism, which is an outcome of Nano AlN particles wide-open over the worn surface and loose fragments amid surfaces. The inclusion of Nano AlN particles repels the delamination process (Figures 13(a)–13(c)). The raise in Nano AlN wt.% from 4 to 12 enhances the wear resistance. It is witnessed that AA6063 matrix and 4 wt.% reinforced Nano AlN composites exposed to extreme plastic deformation compared to 12 wt.% reinforced Nano AlN.

3.12. Drilling Behavior of AA6063-Nano AlN Composites. MRR and SR analysis was done to predict the optimal parameters to acquire higher MRR and SR for manufactured samples through GRA. Tests were conducted with reference to L9 OA. The results are displayed in Table 1.

3.13. Effect of Process Parameter on MRR and SR. Figures 14(a)–14(c) display the contour plot for MRR and SR (a) CS vs. FR, (b) FR vs. DOC, and (c) DOC vs CS. It is perceived that higher MRR and least SR were obtained while improving the feed rate. From Figures 14(a)–14(c), it can be understood that FR 0.25 mm/rev is the major influencing parameter than that of CS and DOC. The MRR and SR is in the order of 3000 > 2000 > 1000 feed rate mm/rev.

3.14. Grey Relational Analysis (GRA). A GRA is a newer technique for estimate, establishing relational examination, and in choice making in various fields of fabrication industries [37]. To acquire higher MRR and SR for drilling of AA6063-Nano AlN composites, appropriate process parameters should be chosen for that GRA is the most suitable optimization process. Table 2 displays the normalized S/N ratio and deviation sequence for MRR and SR. Table 3 shows the GRC, GRG with rank for 9 trials. From Table 3, it is clear that the 9th trial is the optimal one to attain higher MRR and SR. From Table 4, it is seen that 0.2407 is the boundary of max-min regard (Figure 15). From Table 4, it is clear that FR is the substantial parameter tracked by CS and DOC. The series of influencing parameters is in the order as numbered FR (0.2407), CS (0.2130), and DOC (0.3182).

TABLE 3: Evaluated GRC and GRG rank.

Ex. No	GRC		GRG	Rank
	MRR	SR		
1	0.333333	0.532258	0.432796	6
2	0.425287	0.785714	0.605501	4
3	0.560606	0.673469	0.617038	3
4	0.359223	0.434211	0.396717	8
5	0.4625	0.333333	0.397917	7
6	0.616667	0.39759	0.507129	5
7	0.393617	0.362637	0.378127	9
8	0.513889	1	0.756944	2
9	1	0.611111	0.805556	1

TABLE 4: Response table for means.

Level	CS (rpm)	FR (mm/rev)	DOC (mm)
1	0.5518	0.4025	0.5656
2	0.4339	0.5868	0.6026
3	0.6469	0.6432	0.4644
Delta	0.2130	0.2407	0.1382
Rank	2	1	3

3.15. Analysis of Variance. The outcomes of the process parameters inducing several lead features are inspected through ANOVA. To predict the major extensive parameters, ANOVA for GRG is shown in Table 5. It is clearly witnessed from Table 5 that FR is a noteworthy parameter (subsidizing 45.89%). The FR possesses major influence multienactment characteristics for AA6063-Nano AlN composites lagged behind by CS (32.96%) and DOC (14.83%).

4. Conclusions

- (i) AA6063-Nano AlN composite was efficaciously manufactured via SC process
- (ii) The effects of Nano AlN particles on AA6063 matrix on the microstructure and properties were analyzed
- (iii) SEM analysis shows the existence and even dispersal of Nano AlN particles in AA6063 matrix
- (iv) The inclusion of Nano AlN particles with AA6063 enhances the density and reduces the porosity
- (v) The 12 wt.% addition of Nano AlN particles into AA6063 matrix improves the complete mechanical behavior of the composites
- (vi) The tensile fracture analysis was done on the AA6063-Nano AlN composites using SEM
- (vii) The thermal conductivity examination was carried out and stated that the inclusion of Nano AlN particles into AA6063 matrix reduces the thermal conductivity

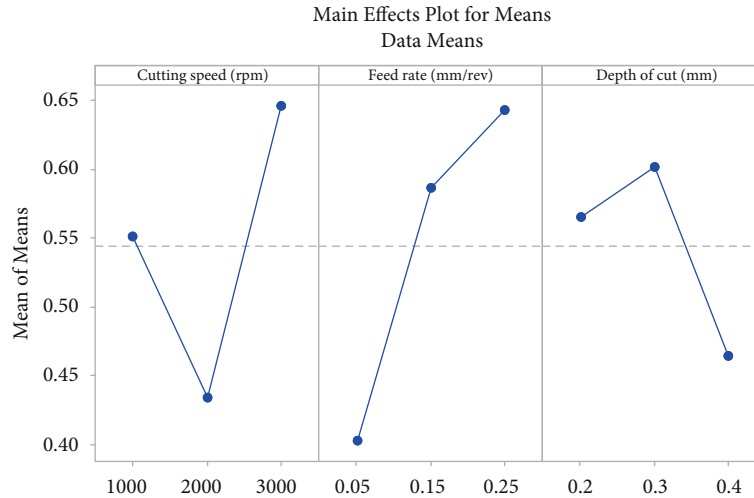


FIGURE 15: Main effects plot for SN ratios.

TABLE 5: ANOVA table.

Source	DF	Seq SS	Adj SS	Adj MS	F	P	Contribution (%)
CS (rpm)	2	0.068284	0.068284	0.034142	5.23	0.161	32.96%
FR (mm/rev)	2	0.095065	0.095065	0.047533	7.27	0.121	45.89%
DOC (mm)	2	0.030728	0.030728	0.015364	2.35	0.298	14.83%
Error	2	0.013068	0.013068	0.006534			
Total	8	0.207146					

$S = 0.0808336$; $R\text{-Sq} = 93.69\%$; $R\text{-Sq}(\text{adj}) = 74.77\%$.

- (viii) The electrical resistivity and electrical conductivity analysis was conducted and found that an increase in Nano AlN particles with AA6063 matrix enhances the electrical resistivity and declines the thermal conductivity
- (ix) Tribological behaviors of AA6063-Nano AlN composites were analyzed and concluded that the inclusion of Nano AlN particles with AA6063 reduces the mass loss
- (x) The worn surface analysis was done on the AA6063-Nano AlN composites via SEM to predict the wear mechanism
- (xi) The CNC drilling behavior of AA6063-Nano AlN composites was studied via GRA and the optimal parameters to acquire higher MRR, and the least SR was determined as FR 0.25 mm/rev, CS 3000 rpm, and DOC 0.3 mm
- (xii) To determine the influencing parameters on the responses FR, CS, and DOC, ANOVA was utilized

Data Availability

The data used to support the findings of this study are included in the article.

Conflicts of Interest

The authors declare that there is no conflict of interest regarding the publication of this paper.

Acknowledgments

The authors thank the Bharath Institute of Higher Education and Research and K. Ramakrishnan College of Engineering for providing facilities support to complete this research work. The authors also thank the AMIT, Arbaminch University, Ethiopia, and Pusan National University, South Korea, for providing help during the research and preparation of the manuscript. This project was supported by Researchers Supporting Project number (RSP-2021/332), King Saud University, Riyadh, Saudi Arabia.

References

- [1] S. Chand, P. Chandrasekhar, S. Roy, and S. Singh, "Influence of dispersoid content on compressibility, sinterability and mechanical behaviour of B4C/BN reinforced Al6061 metal matrix hybrid composites fabricated via mechanical alloying," *Metals and Materials International*, vol. 27, no. 11, pp. 4841–4853, 2021.
- [2] N. Singh, R. M. Belokar, and R. S. Walia, "A critical review on advanced reinforcements and base materials on hybrid metal matrix composites," *Silicon*, pp. 1–24, 2020.

- [3] A. Mahato and S. Mondal, "Fabrication and microstructure of micro and nano silicon carbide reinforced copper metal matrix composites/nanocomposites," *Silicon*, vol. 13, pp. 1097–1105, 2021.
- [4] S. I. Gad, M. A. Attia, M. A. Hassan, and A. G. El-Shafei, "Predictive computational model for damage behavior of metal-matrix composites emphasizing the effect of particle size and volume fraction," *Materials*, vol. 14, no. 9, p. 2143, 2021.
- [5] B. Hekner, J. Myalski, P. Wrześniowski, and T. Maciąg, "Al matrix composites reinforced by Ti and C dedicated to work at elevated temperature," *Materials*, vol. 14, no. 11, p. 3114, 2021.
- [6] B. Gobalakrishnan, C. Rajaravi, G. Udhayakumar, and P. R. Lakshminarayanan, "Effect of ceramic particulate addition on aluminium based ex-situ and in-situ formed metal matrix composites," *Metals and Materials International*, vol. 27, no. 9, pp. 3695–3708, 2021.
- [7] A. Kareem, J. A. Qudeiri, A. Abdudeen, T. Ahammed, and A. Ziout, "A review on AA 6061 metal matrix composites produced by stir casting," *Materials*, vol. 14, no. 1, p. 175, 2021.
- [8] V. Mohanavel, "Synthesis and evaluation on mechanical properties of LM4/AlN alloy based composites," *Energy Sources, Part A: Recovery, Utilization, and Environmental Effects*, vol. 2019, article 1647313, 8 pages, 2019.
- [9] H. Yu, H. Chen, R. Ma, and G. Min, "Fabrication of AlN-TiC/Al composites by gas injection processing," *Rare Metals*, vol. 25, no. 6, pp. 659–664, 2006.
- [10] K. Sanesh, S. S. Sunder, and N. Radhika, "Effect of reinforcement content on the adhesive wear behavior of Cu₁₀Sn₅Ni/Si₃N₄ composites produced by stir casting," *Metallurgy and Materials*, vol. 24, no. 9, pp. 1052–1060, 2017.
- [11] R. Nithesh, N. Radhika, and S. Shiam Sunder, "Mechanical properties and adhesive scuffing wear behaviour of stir cast Cu-Sn-Ni/Si₃N₄ composites," *Journal of Tribology*, vol. 139, no. 6, 2017.
- [12] J. S. D. Joseph, B. Kumaragurubaran, and S. Sathish, "Effect of MoS₂ on the wear behavior of aluminium (AlMg0.5Si) composite," *Silicon*, vol. 12, no. 6, pp. 1481–1489, 2020.
- [13] S. Saravanan, P. Senthilkumar, M. Ravichandran, and V. Anandakrishnan, "Mechanical, electrical, and corrosion behavior of AA6063/TiC composites synthesized via stir casting route," *Journal of Materials Research*, vol. 32, no. 3, pp. 606–614, 2017.
- [14] V. Mohanavel and M. Ravichandran, "Experimental investigation on mechanical properties of AA7075-AlN composites," *Materials Testing*, vol. 61, no. 6, pp. 554–558, 2019.
- [15] B. A. KUMAR, N. MURUGAN, and I. DINAHARAN, "Dry sliding wear behavior of stir cast AA6061-T6/AlN_p composite," *Transactions of Nonferrous Metals Society of China*, vol. 24, no. 9, pp. 2785–2795, 2014.
- [16] M. Zhao, G. Wu, D. Zhu, L. Jiang, and Z. Dou, "Effects of thermal cycling on mechanical properties of AlNp/Al composite," *Material Letters*, vol. 58, no. 12-13, pp. 1899–1902, 2004.
- [17] V. M. Kumar and C. V. Venkatesh, "Evaluation of microstructure, physical and mechanical properties of Al 7079 – AlN metal matrix composites," *Materials Research Express*, vol. 6, no. 12, article 126503, 2019.
- [18] S. Fale, A. Likhite, and J. Bhatt, "Compressive, tensile and wear behavior of ex situ Al/AlN metal matrix nanocomposites," *Journal of Composite Materials*, vol. 49, no. 16, pp. 1917–1928, 2015.
- [19] E. A. M. Shalaby and A. Y. Churyumov, "Development and characterization of A359/AlN composites for automotive applications," *Journal of Alloys and Compounds*, vol. 727, pp. 540–548, 2017.
- [20] N. Radhika and R. Raghu, "Abrasive wear behavior of monolithic alloy, homogeneous and functionally graded aluminum (LM25/AlN and LM25/SiO₂) composites," *Particulate Science and Technology An International Journal*, vol. 37, no. 1, pp. 10–20, 2019.
- [21] N. Radhika and R. Raghu, "Investigation on mechanical properties and analysis of dry sliding wear behavior of Al LM13/AlN metal matrix composite based on Taguchi's technique," *Journal of Tribology*, vol. 139, no. 4, article 041602, 2017.
- [22] S. Basavarajappa, G. Chandramohan, J. P. Davim et al., "Drilling of hybrid aluminium matrix composites," *International Journal of Advanced Manufacturing Technology*, vol. 35, no. 11-12, pp. 1244–1250, 2008.
- [23] T. Rajmohan and K. Palanikumar, "Modeling and analysis of performances in drilling hybrid metal matrix composites using D-optimal design," *International Journal of Advanced Manufacturing Technology*, vol. 64, no. 9-12, pp. 1249–1261, 2013.
- [24] T. Rajmohan, K. Palanikumar, and M. Kathirvel, "Optimization of machining parameters in drilling hybrid aluminium metal matrix composites," *Transactions of the Nonferrous Metals Society of China*, vol. 22, article 12861297, 2012.
- [25] M. Elango and K. Annamalai, "High speed machining and optimisation of Al/SiC/Gr hybrid metal matrix composites using ANOVA and grey relational analysis," *Australian Journal of Mechanical Engineering*, vol. 2020, article 1761587, 12 pages, 2020.
- [26] Y. Altunpak, M. Ay, and S. Aslan, "Drilling of a hybrid Al/SiC/Gr metal matrix composites," *International Journal of Advanced Manufacturing Technology*, vol. 60, no. 5-8, pp. 513–517, 2012.
- [27] K. K. Alaneme and M. O. Bodunrin, "Mechanical behaviour of alumina reinforced aa6063 metal matrix composites developed by two-step – stir-casting process, acta technica corviniensis bulletin of engineering," *Acta Technica Corviniensis-bulletin of engineering*, vol. 6, no. 3, p. 105, 2013.
- [28] T. Anandaraj, P. P. Sethusundaram, M. Meignanamoorthy, and M. Ravichandran, "Investigations on properties and tribological behavior of AlMg4.5Mn0.7(AA5083)-MoO₃ composites prepared by stir casting method," *Surface Topography: Metrology and Properties*, vol. 9, no. 2, article 025011, 2021.
- [29] R. Jojith and N. Radhika, "Mechanical and tribological properties of LM13/TiO₂/MoS₂ hybrid metal matrix composite synthesized by stir casting," *Particulate Science and Technology*, vol. 37, no. 5, pp. 570–582, 2019.
- [30] G. K. Meenashisundaram, S. Seetharaman, and M. Gupta, "Enhancing overall tensile and compressive response of pure Mg using nano- TiB₂ particulates," *Materials characterization*, vol. 94, pp. 178–188, 2014.
- [31] B. Kuldeep, K. P. Ravikumar, S. Pradeep, and K. R. Gopi, "Effect of boron nitride and zirconium dioxide on mechanical behavior of Al7075 metal matrix hybrid composite," *Materials Research Express*, vol. 6, no. 3, article 036509, 2019.
- [32] E. Nas and H. Gokkaya, "Mechanical and physical properties of hybrid reinforced (Al/B4C/Ni(K)Gr) composite materials

- produced by hot pressing,” *Materials Testing*, vol. 57, no. 6, pp. 524–530, 2016.
- [33] P. Zhang, J. Jie, Y. Gao et al., “Preparation and properties of TiB₂ particles reinforced Cu-Cr matrix composite,” *Materials Science and Engineering A*, vol. 642, pp. 398–405, 2015.
- [34] B. Stalin, G. T. Sudha, and M. Ravichandran, “Investigations on characterization and properties of Al-MoO₃ composites synthesized using powder metallurgy technique,” *Silicon*, vol. 10, no. 6, pp. 2663–2670, 2018.
- [35] G. S. Pradeep Kumar and R. Keshavamurthy, “Corrosion behaviour of TiB₂ reinforced aluminium based in situ metal matrix composites,” *Perspectives in Science*, vol. 8, pp. 172–175, 2016.
- [36] S. Arivukkarasan, V. Dhanalakshmi, B. Stalin, and M. Ravichandran, “Mechanical and tribological behaviour of tungsten carbide reinforced aluminum LM4 matrix composites,” *Particulate Science and Technology*, vol. 36, no. 8, pp. 967–973, 2018.
- [37] S. Singh, I. Singh, and A. Dvivedi, “Multi objective optimization in drilling of Al6063/10% SiC metal matrix composite based on grey relational analysis,” *Journal of Engineering Manufacture.*, vol. 227, no. 12, pp. 1767–1776, 2013.